Journal of Pharmaceutical and Biomedical Analysis 55 (2011) 31–47

Contents lists available at ScienceDirect

Journal of Pharmaceutical and Biomedical Analysis

journal homepage: www.elsevier.com/locate/jpba

Gradient RP-HPLC method for the determination of potential impurities in atazanavir sulfate

Sreenivasa Rao Chitturi[a], Yallappa Somappa Somannavar[a], Badarinadh Gupta Peruri[a], Sreenivas Nallapati[a], Hemant Kumar Sharma[a,*], Shankar Reddy Budidet[a], Vijay Kumar Handa[a], Hima Bindu Vurimindi[b]

[a] APL Research Centre (A Division of Aurobindo Pharma Limited), 313, Bachupally, Hyderabad 500 090, Andhra Pradesh, India
[b] Centre for Environment, Institute of Science and Technology, Jawaharlal Nehru Technological University, Kukatpally, Hyderabad 500 085, Andhra Pradesh, India

ARTICLE INFO

Article history:
Received 28 May 2010
Received in revised form
24 December 2010
Accepted 10 January 2011
Available online 19 January 2011

Keywords:
Atazanavir sulfate
Isolation and characterization
Method development and validation
Order of reaction
Potential impurities

ABSTRACT

This paper proposes a simple and selective RP-HPLC method for the determination of process impurities and degradation products (degradants) of atazanavir sulfate (ATV) drug substance. Chromatographic separation was achieved on Ascentis® Express C8, (150 mm × 4.6 mm, 2.7 μm) column thermostated at 30 °C under gradient elution by a binary mixture of potassium dihydrogen phosphate (pH 3.5, 0.02 M) and ACN at a flow rate of 1.0 ml/min. A photodiode array (PDA) detector set at 250 nm was used for detection. Stress testing (forced degradation) of ATV was carried out under acidic, alkaline, oxidative, photolytic, thermal and humidity conditions. In presence of alkali, ATV transformed into cyclized products and the order of degradation reaction is determined by the method of initial rates. The unknown process impurities and alkaline degradants are isolated by preparative LC and characterized by ESI-MS/MS, ^{1}H NMR, and FT-IR spectral data. The developed method is validated with respect to sensitivity (lod and loq), linearity, precision, accuracy and robustness and can be implemented for routine quality control analysis and stability testing of ATV.

1. Introduction

Atazanavir sulfate is an azapeptide inhibitor of HIV-1 protease [1]. Atazanavir sulfate (ATV) is chemically designated as (3S,8S,9S,12S)-3,12-bis(1,1-dimethylethyl)-8-hydroxy-4,11-dioxo-9-(phenylmethyl)-6-[[4-(2-pyridinyl)phenyl]methyl]-2,5,6,10,13-pentaazatetradecanedioic acid dimethyl ester, sulfate (1:1) (Fig. 1). The compound selectively inhibits the virus-specific processing of viral Gag and Gag-Pol polyproteins in HIV-1 infected cells, thus preventing formation of mature virions. ATV is distinguished from other protease inhibitors in that it can be given once-daily and has lesser effects on the patient's lipid profile. It is the first protease inhibitor approved by United States Food and Drug Administration (USFDA) and marketed under the trade name of REYATAZ (capsule formulation) by Bristol-Myers.

Several research papers have been reported in the literature for the determination of ATV [2–23]. These are the test methods related to the determination of ATV alone and concurrently with other antiretrovirals in human plasma and other biological stuff, based on LC/MS/MS [2–11] and HPLC [12–23]. Seshachalam et al. [13] have reported a stability indicating HPLC method for the assay of ATV in the presence of degradation products (degradants), which described an isocratic RP-HPLC method. However, this paper was restricted to the determination of ATV only from its degradants and the details of degradants formed under the stress conditions employed were neither discussed nor characterized. To the best of our knowledge, a complete validated HPLC method for the determination of impurities of ATV either in bulk drug substances or in finished pharmaceutical products is not reported till date. Further, no monograph on ATV is published in any of the pharmacopoeia for compendial applications. During the analysis of lab batches from synthetic process development of ATV, the impurities RS1, RS2, RS3, RS4, RS5, RS6, RS7, RS10, RS11, RS12 and RS13 are found as process related (Fig. 1) of which RS3, RS10 and RS12 are unknown impurities. The levels of detected impurities are ranged from 0.02 to 0.2 area percent (AP). So, a comprehensive study is undertaken to isolate and characterize these impurities by spectroscopic techniques. Stress testing (forced degradation) of ATV was carried out under hydrolytic (acid/alkaline),

Abbreviations: ATV, atazanavir sulfate; PDA, photodiode array; AP, area percent; OPA, orthophosphoric acid; CF, correction factor.

* Corresponding author at: Analytical Research Division, APL Research Centre (A Division of Aurobindo Pharma Limited), 313, Bachupally, Hyderabad 500090, Andhra Pradesh, India. Tel.: +91 40 23040263; fax: +91 40 23042932.
E-mail addresses: hemant@aurobindo.com, ard@aurobindo.com (H.K. Sharma).

0731-7085/$ – see front matter © 2011 Elsevier B.V. All rights reserved.
doi:10.1016/j.jpba.2011.01.002

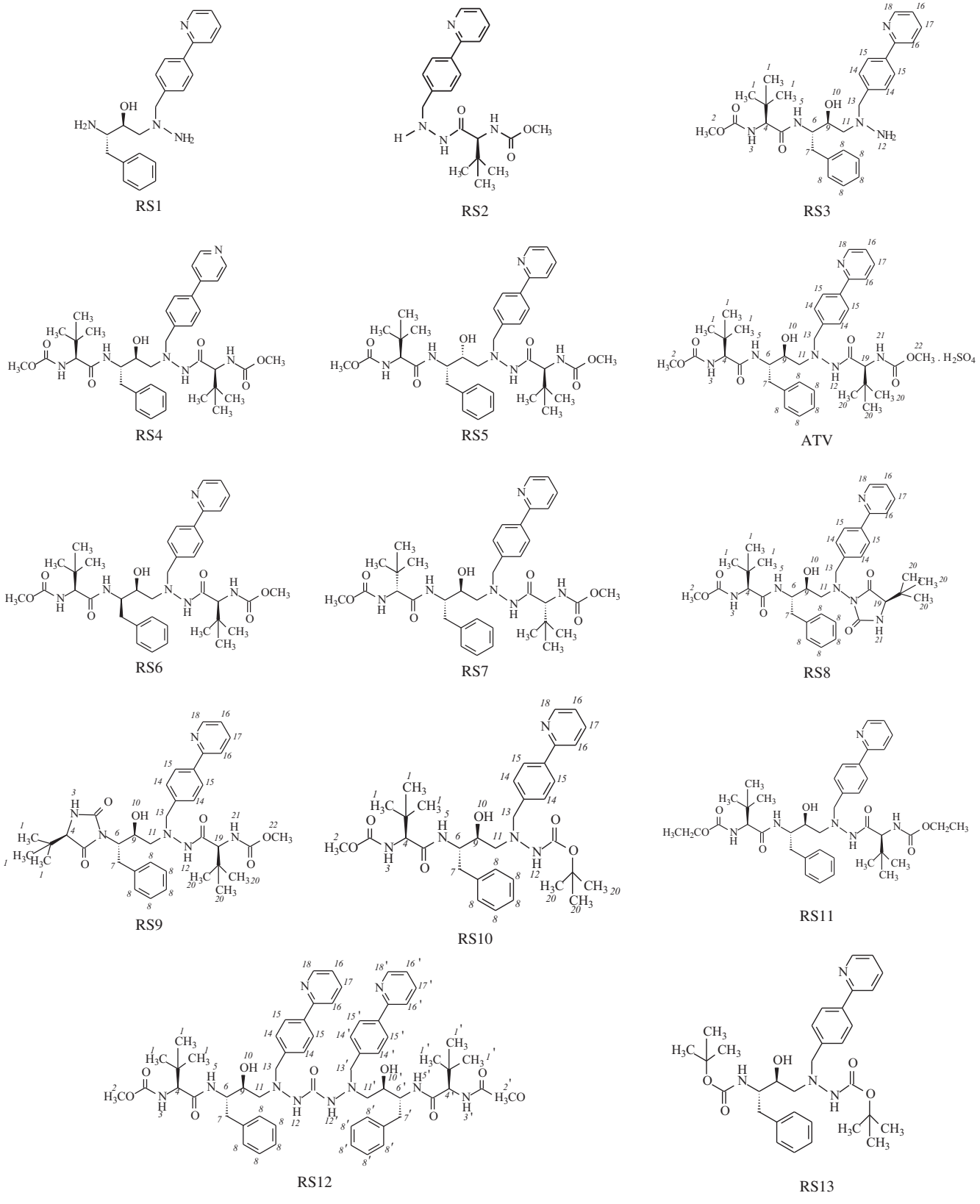

Fig. 1. Chemical structures of ATV and its impurities (RS1, RS2, RS3, RS4, RS5, RS6, RS7, RS8, RS9, RS10, RS11, RS12 and RS13).

oxidative, thermal, photolytic and humidity conditions [24]. Two cyclization degradants (RS8 and RS9) (Fig. 1) are formed under alkaline stress, whose isolation and characterization is not reported. In the present study kinetics of the degradation is also discussed.

As per the requirements of regulatory authorities, the impurity profile study of drug substances and drug products has to be carried out using a suitable analytical method in the final product [25,26]. The unknown impurities (RS3, RS8, RS9, RS10 and RS12) are isolated and characterized by ESI-MS/MS, ^{1}H NMR and FT-IR spectral data.

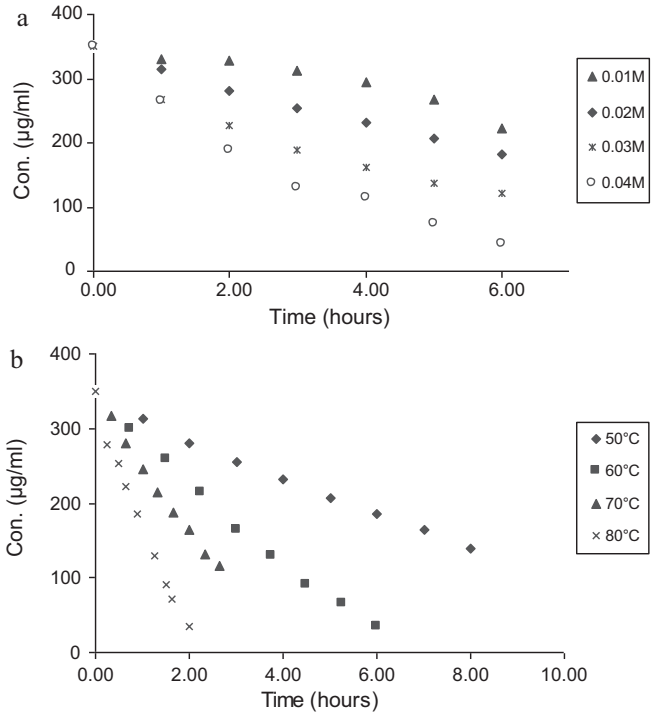

Fig. 2. The effect of (a) concentration of NaOH and (b) temperature on the degradation of ATV.

We herein describe the development and validation of a simple RP-HPLC method in gradient elution mode for the determination of potential process related impurities and degradants in ATV drug substance.

2. Experimental

2.1. Materials and reagents

Analytical grade potassium dihydrogen orthophosphate, ammonium acetate, hydrochloric acid, sodium hydroxide and hydrogen peroxide (Merck, Mumbai, India), HPLC grade water (Millipore, Milford, MA, USA) was used throughout the analysis. Orthophosphoric acid (OPA) was obtained from Fluka chemicals, Switzerland. The investigated samples of ATV drug substance, crude samples and impurities were synthesized in APL Research Centre, Hyderabad.

2.2. Apparatus and conditions

2.2.1. Preparative HPLC

A Shimadzu LC-8A Preparative LC equipped with SPD-10A VP, UV-VIS detector (Shimadzu Corporation, Analytical Instruments Division, Kyoto, Japan) was used. Peerless Basic C18 and Hyperprep HS C18 (500 mm × 30 mm, particle size 10 μm) columns were employed for separation and isolation of impurities using water/ammonium acetate (0.025 M) as mobile phase A and ACN as mobile phase B with varying compositions and flow rate of 25–35 ml/min and detection was carried out at 250 nm.

2.2.2. Mass spectrometry

An Applied Biosystems triple quadrupole mass spectrometer (API 2000 LC/MS/MS, MDS SCIEX, Foster City, CA, USA) equipped with a Turbo ion spray interface was used. The data acquisition and processing was carried out by Analyst software. The typical source conditions were: capillary voltage, 5.5 kV; temperature, 375 °C; curtain gas (N_2) flow rate, 20 units; declustering potential, 40 V; focusing potential, 350 V, entrance potential, 10 V; collision energy, 35 eV; collision exit potential, 30 eV and CAD flow rate, 2 l/min.

2.2.3. ^{1}H NMR spectroscopy

The ^{1}H NMR spectra were recorded on a Bruker 300 MHz NMR Spectrometer (Bruker BioSpin AG, Faellanden, Switzerland) at room temperature, 22 °C using DMSO-d_6 as solvent and tetramethylsilane (TMS) as internal standard. The data acquisition and processing was carried out by XWIN-NMR software. The ^{1}H NMR chemical shifts were reported on the d scale in ppm relative TMS (δ = 0.00).

2.2.4. FT-IR spectroscopy

The FT-IR spectra were recorded as KBr pellets using PerkinElmer Spectrum One FT-IR Spectrometer (PerkinElmer Life and Analytical Sciences, Shelton, CT, USA).

2.2.5. HPLC

The HPLC systems used in this study were

(i) Waters HPLC (Milford, MA, USA) equipped with Alliance 2695 separations module, 996 photodiode array (PDA) detector with Empower software.
(ii) Shimadzu *VP* series liquid chromatograph (Shimadzu Corporation, Analytical Instruments Division, Kyoto, Japan) equipped SCL-10A system controller with Class *VP* software, LC-10AT pumps (binary) with gradient mixer assembly, SIL-10AD auto injector, CTO-10AS column oven and SPD UV-VIS detector.
(iii) Agilent HPLC 1100 series (Agilent Technologies, Deutschland GmbH, Waldbronn, Germany) with chemstation software equipped with, G1379A degasser, G1311A quaternary pump, G1367A auto injector, G1330B sample cooler, G16A column oven and G1315B DAD detector.

The HPLC columns used in this study were

(i) Symmetry C8, 150 mm × 4.6 mm, 3 μm (Waters Corporation, USA).

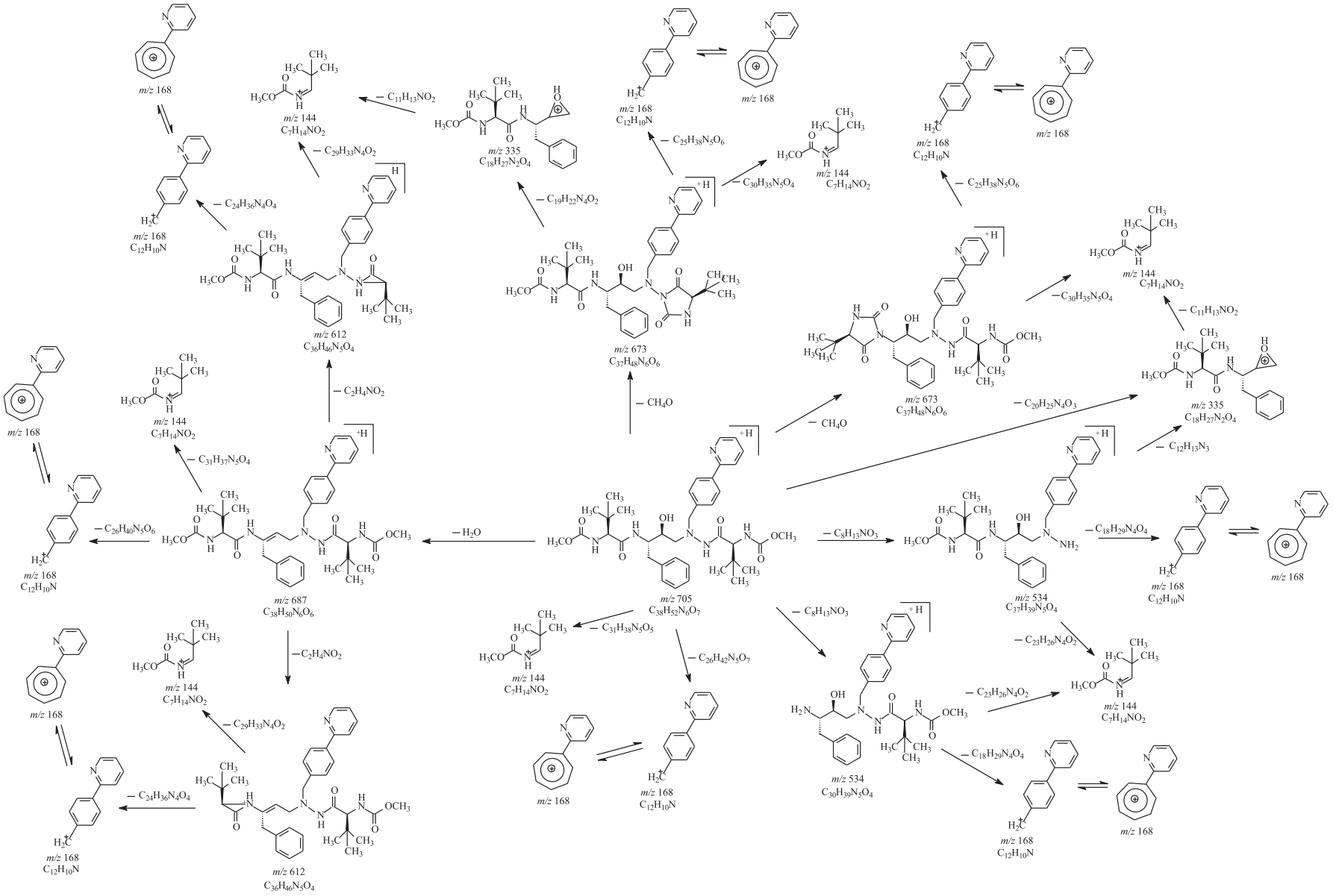

Fig. 3. ESI-MS/MS fragmentation patterns for (a) ATV, (b) RS3, (c) RS8, (d) RS9, (e) RS10 and (f) RS12.

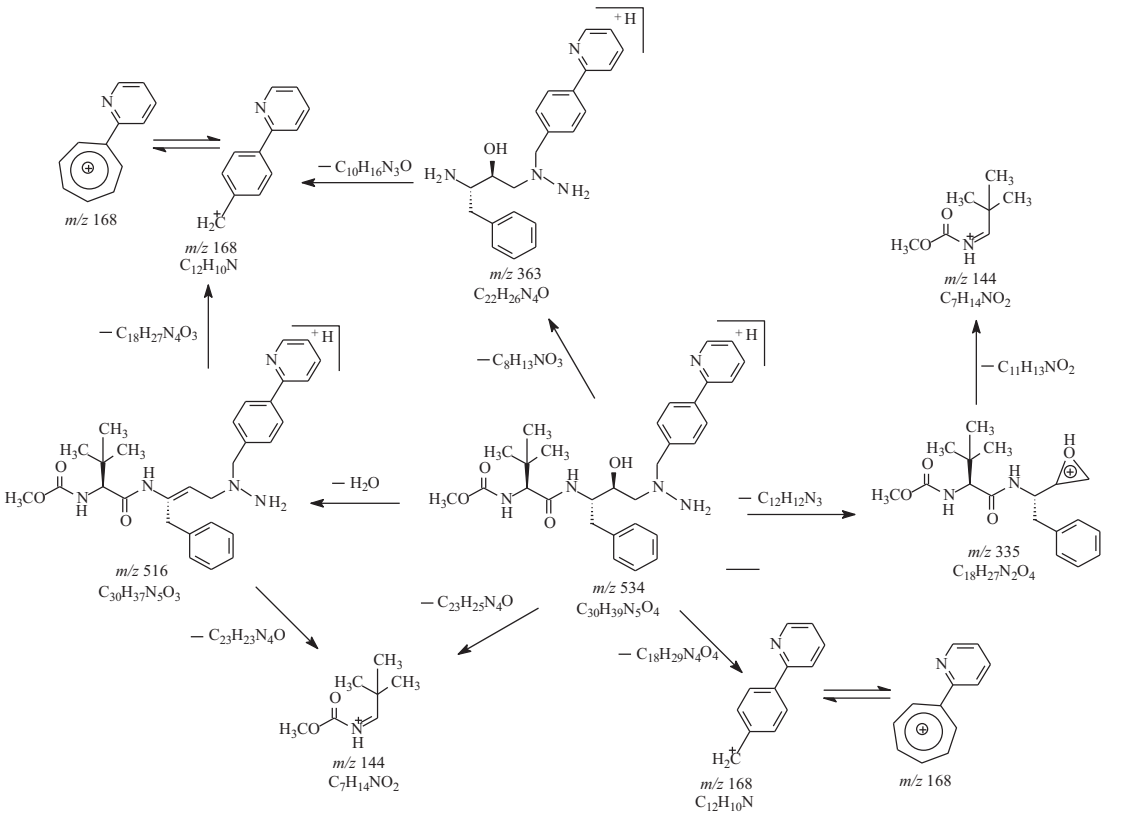

(b) RS3

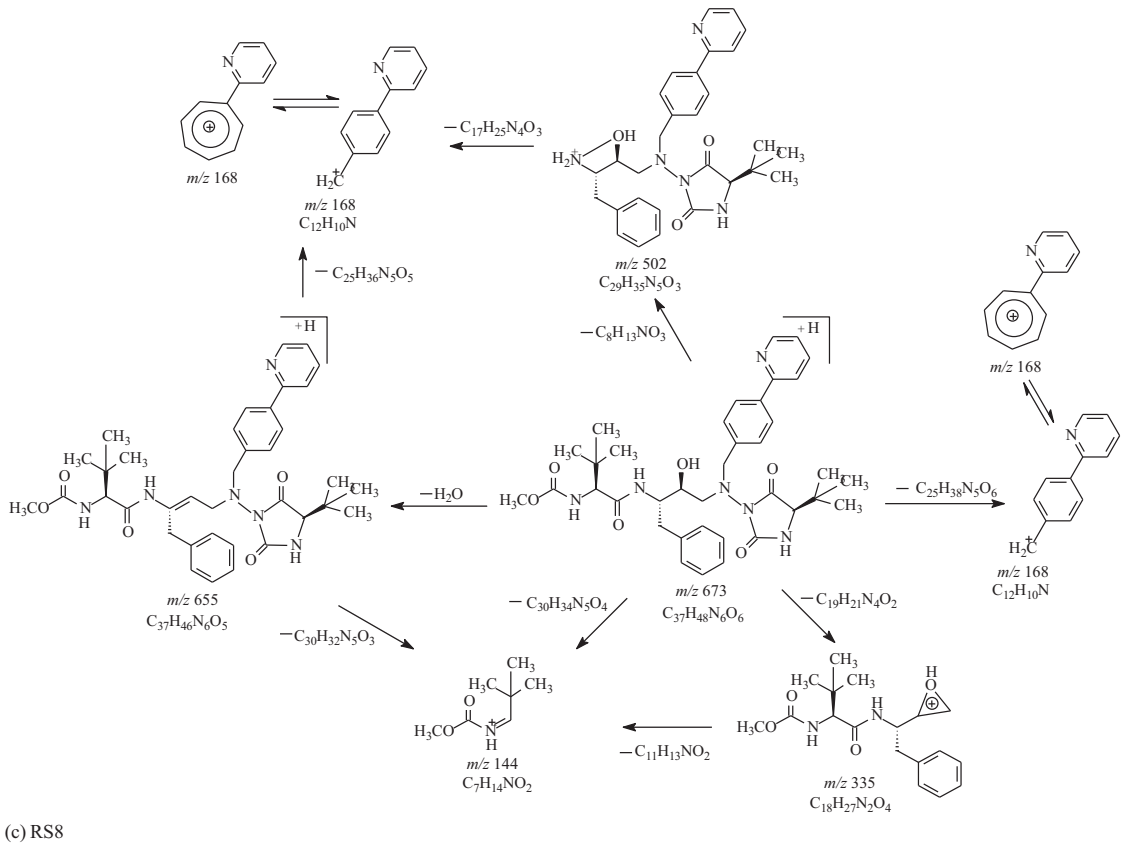

(c) RS8

Fig. 3. (*Continued*).

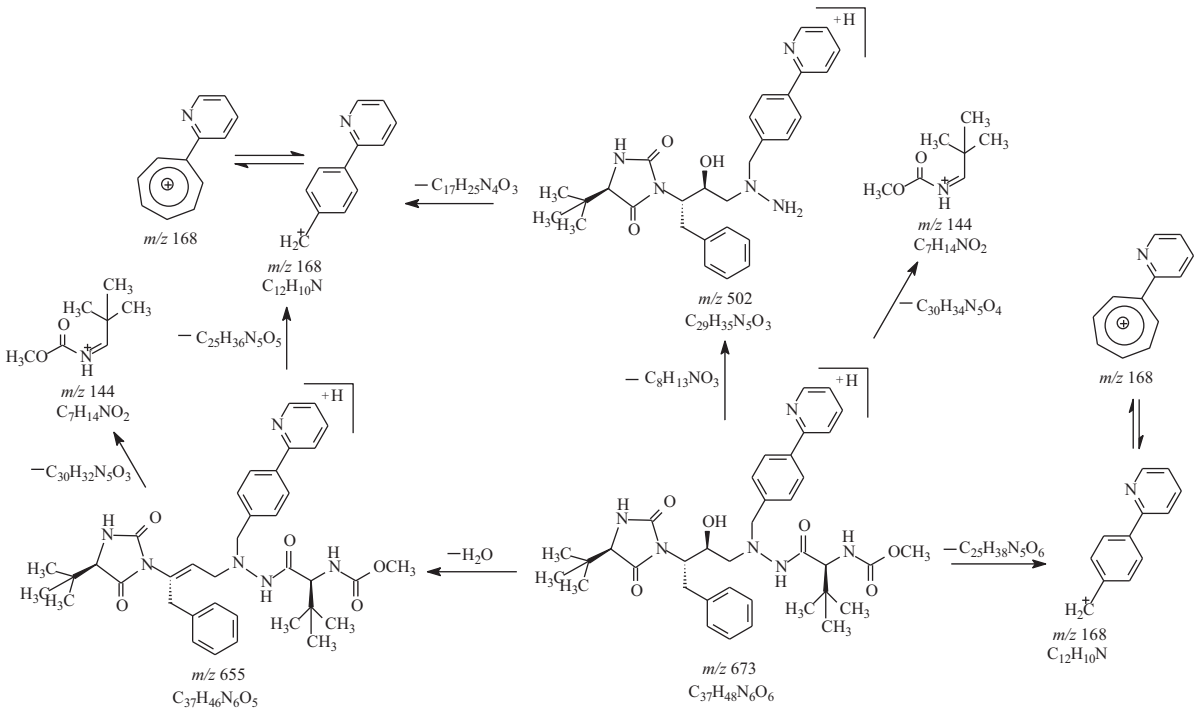

(d) RS9

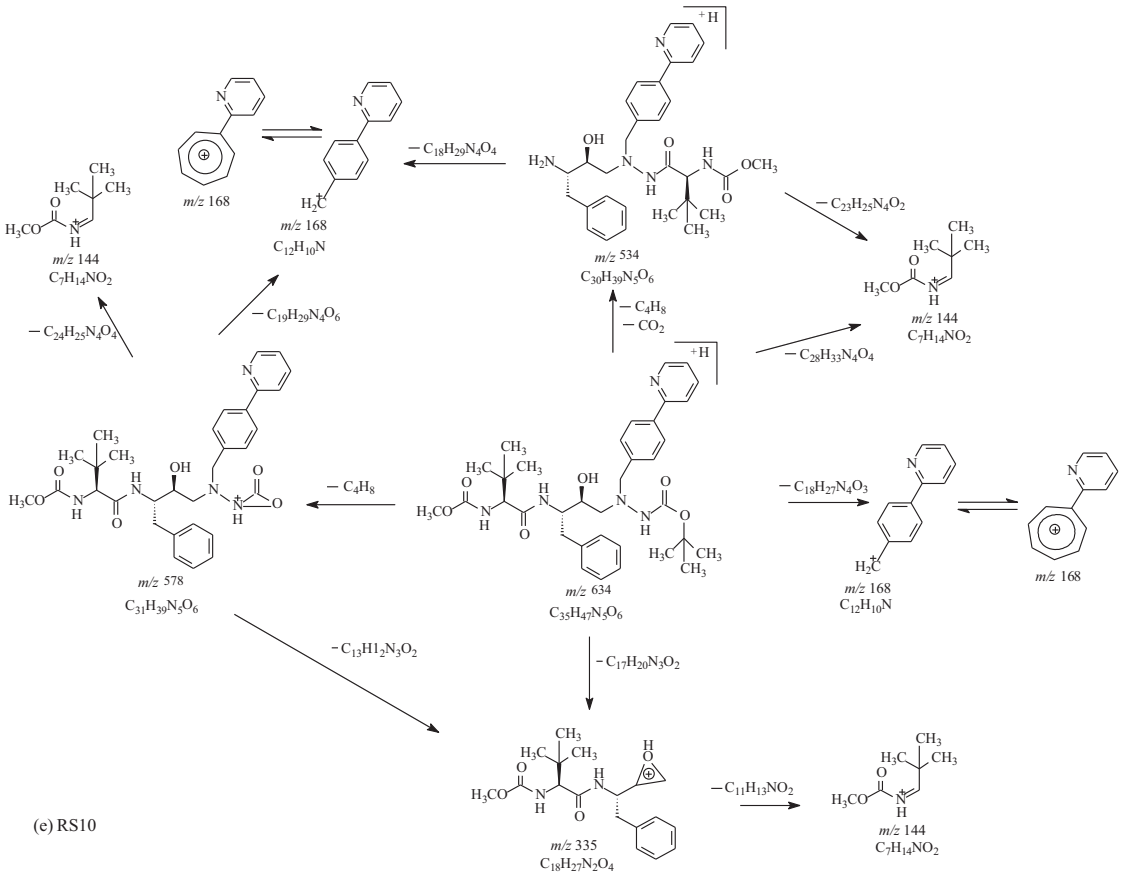

(e) RS10

Fig. 3. (*Continued*).

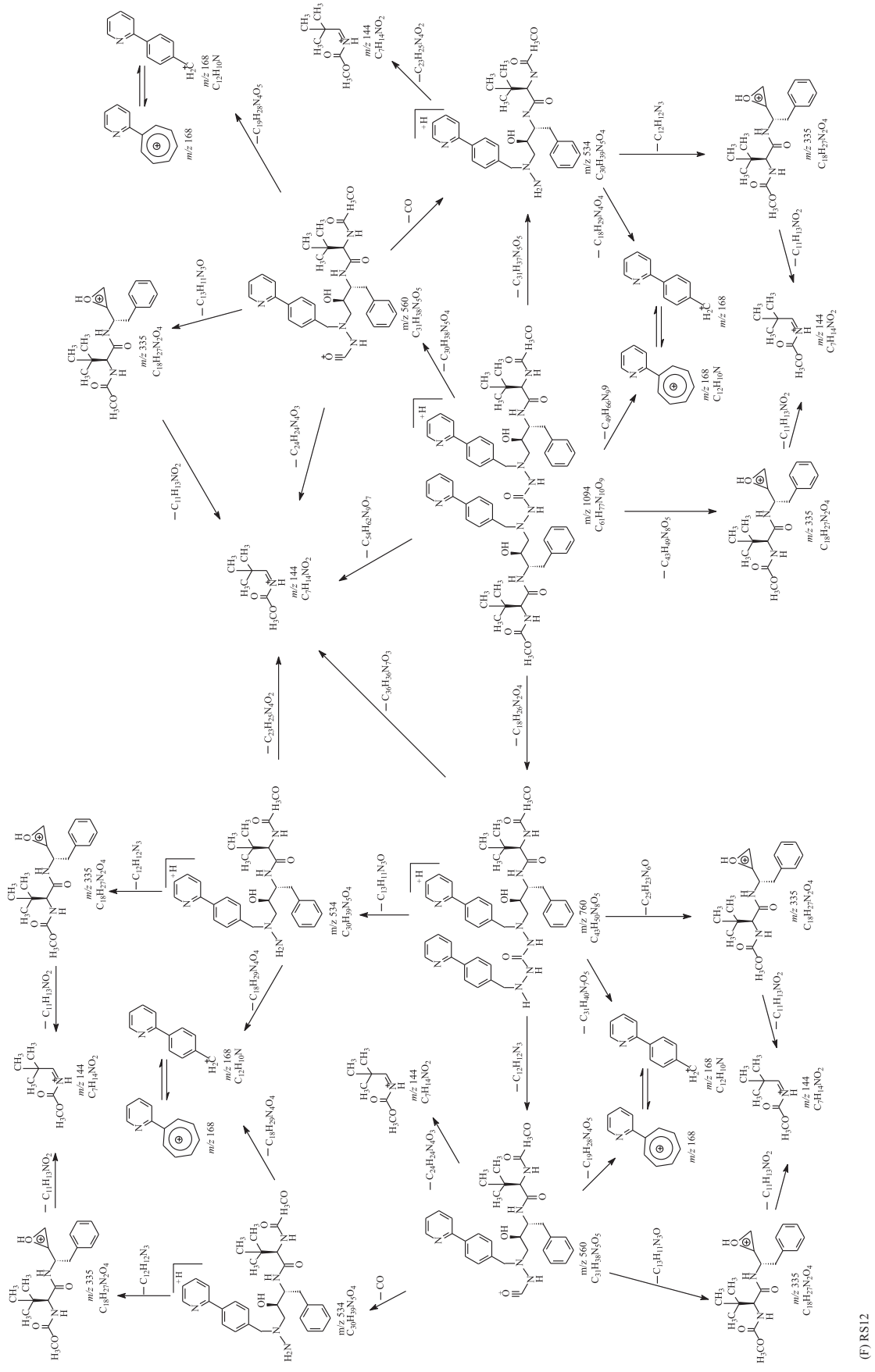

(F) RS12

Fig. 3. (*Continued*).

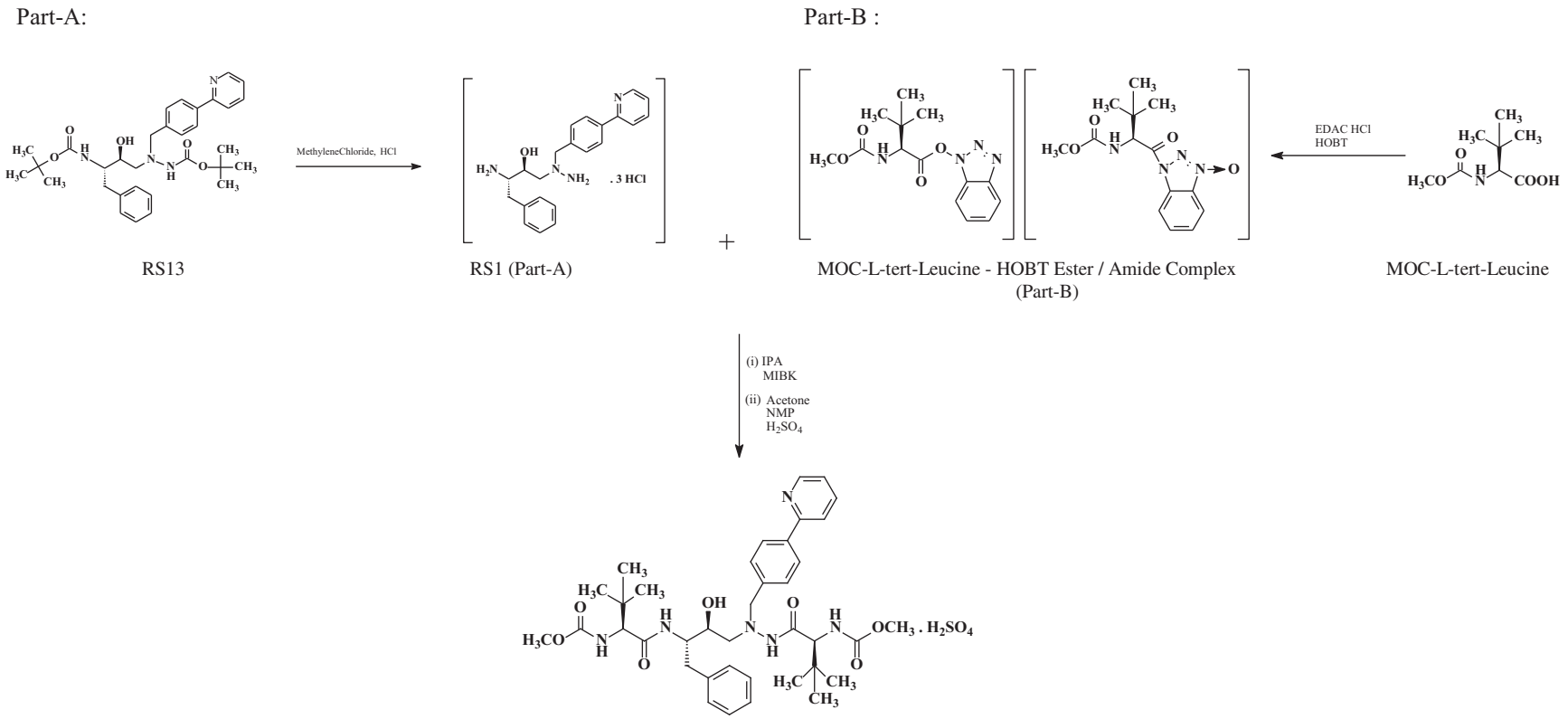

Fig. 4. Reaction scheme for the synthesis of ATV.

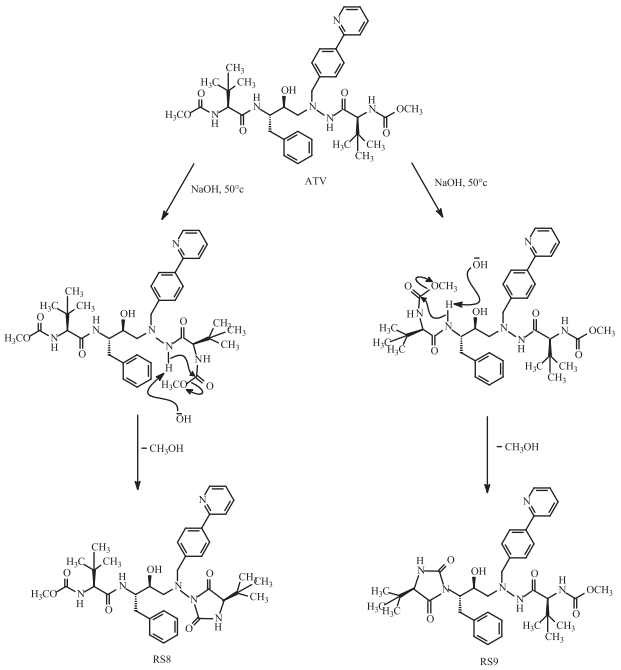

(a) Formation of RS8 & RS9

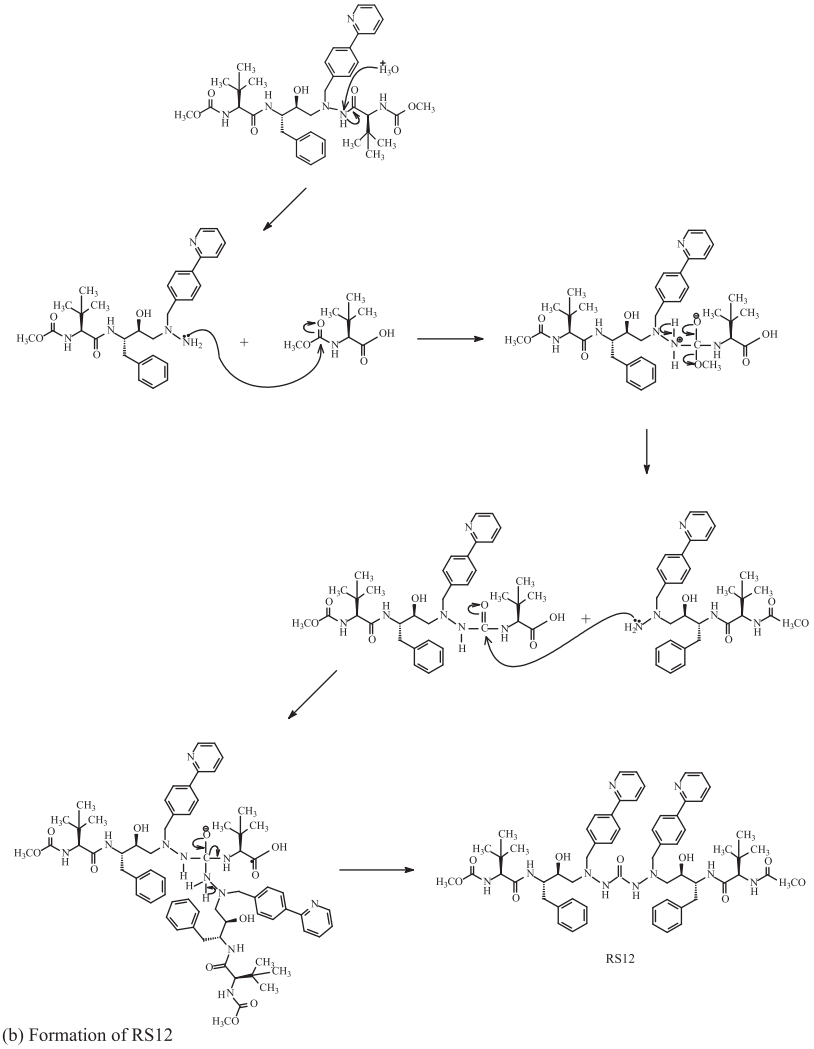

(b) Formation of RS12

Fig. 5. Degradation pathway for ATV under alkaline hydrolysis and for formation of RS12.

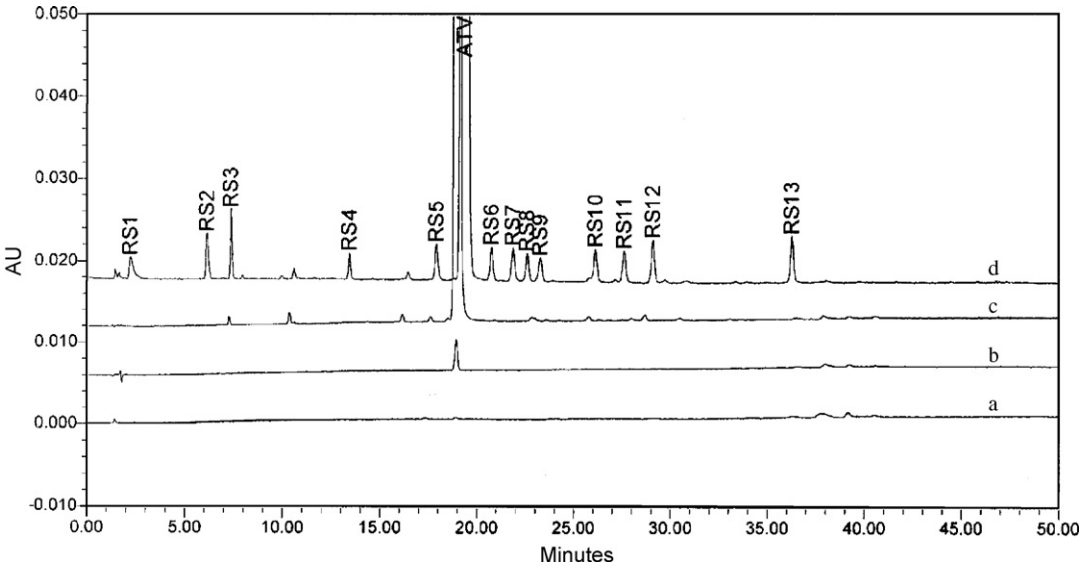

Fig. 6. Typical HPLC chromatograms of (a) diluent, (b) standard, (c) ATV (1140 μg/ml) and (d) ATV (1140 μg/ml) spiked with 0.2% w/w of each impurity using optimized method (column: Ascentis® Express C8, 150 mm × 4.6 mm, 2.7 μm, kept at 30 °C, mobile phases: A: KH_2PO_4 buffer (pH 3.5, 0.02 M), B: ACN, gradient program, 0 min 27% B; 0–10 min 40% B; 10–30 min 50% B; 30–45 min 70% B; 45–50 min 70% B; 50–52 min 27% B and 52–60 min 27% B, flow rate: 1.0 ml/min, injection volume: 20 μl, UV detection: 250 nm).

(ii) YMC Pack C8, 150 mm × 4.6 mm, 3 μm (YMC Inc., USA).
(iii) Ascentis® Express C8, 150 mm × 4.6 mm, 2.7 μm (Sigma–Aldrich, USA) and
(iv) Hypersil BDS C8, 150 mm × 4.6 mm, 3 μm (Thermo Electron Corporation, UK).

The analysis was carried out on Ascentis® Express C8 (150 mm × 4.6 mm, 2.7 μm) column thermostated at 30 °C. The solvent A was potassium dihydrogen orthophosphate buffer (0.02 M KH_2PO_4, pH adjusted to 3.5 with OPA) and solvent B is ACN. Solvent A was filtered through PVDF 0.45 μm membrane filter and degassed prior to pumping into the system along with solvent B. The mobile phase flow rate was 1.0 ml/min. The HPLC gradient program was time (min)/%B (v/v): 0/27, 10/40, 30/50, 45/70, 50/70, 52/27 and 60/27. The injection volume was 20 μl. The chromatograms were recorded at 250 nm using a PDA detector.

2.3. Analytical procedure

ATV working reference standard at 2.3 μg/ml and ATV at 1140 μg/ml concentrations prepared in diluent H_2O/ACN (90:10 v/v) were used as standard and sample solutions respectively. Solutions of all the impurities (0.2 mg/ml) were prepared by dissolving known amounts of the compounds initially in acetonitrile and diluted up to the mark with diluent. These solutions were prepared freshly and diluted further quantitatively to study the validation attributes. The specification limit considered for validation studies was 0.2% for each impurity. Known and unknown impurities were determined against mean areas obtained from six replicate injections of standard solution and correction factors (CF, for a given impurity) were calculated against ATV as the ratio of slope of ATV to slope of respective impurity obtained from the regression line.

2.4. Procedure for forced degradation study

To demonstrate stability-indicating power of developed method for the determination of impurities in ATV, solution-state forced degradation of ATV was carried out by treating the 0.2 mg/ml solutions with 5 M HCl, 0.025 M NaOH and 30% H_2O_2 at 85 °C for 120 min, 15 min and 120 min respectively. Solid state forced degradation (thermal, photolytic and humidity) of the drug was conducted by exposing ATV to (1) heat at 105 °C for 120 h, (2) white fluorescent light of 1.2×10^6 lux followed by UV light of 200 w-h/m^2 and (3) 90% R.H. at 25 °C for 120 h. All these solutions were analyzed by the developed method. Two degradants (RS8 and RS9) were formed under alkaline degradation (Fig. 5) and separated from one another and close eluting impurities. These two degradants have not been reported until now. Further studies are carried out on the effect of concentration of NaOH and temperature to study the kinetics of degradation of ATV.

2.4.1. Kinetic investigation of alkaline degradation

The kinetics of degradation of ATV were explored by studying the effect of concentration of NaOH and effect of temperature. A series of solutions of ATV (350 μg/ml) are treated with different concentrations of NaOH (0.01, 0.02, 0.03, 0.04 M) at the temperature of 50 °C. The analysis was carried out at regular intervals of time and the rate of degradation was observed to increase with increase in NaOH molarity (Fig. 2a). Effect of temperature on rate of degradation was studied in the range of 50–80 °C at 0.02 M NaOH concentration and the degradation rate increased with temperature (Table 1a and Fig. 2b). Order of degradation reaction was determined by the method of initial rates, which were measured at different concentrations of ATV (350 μg/ml and 700 μg/ml) and NaOH (0.02 M and 0.04 M NaOH) (Table 1b).

$$\text{Rate of reaction } (v) = k[\text{ATV}]^a[\text{NaOH}]^b \text{ mol L}^{-1} \text{ min}^{-1}$$

where v is rate of reaction and k is reaction constant, [ATV] and [NaOH] are concentrations of ATV and NaOH respectively. The powers a and b are order of reaction with respect to ATV and NaOH respectively.

2.5. Isolation of process impurities and degradation products

The process impurities RS3, RS10 and RS12 were present in the crude samples at about 0.13–0.3 AP and were isolated by preparative HPLC as per the conditions described in Section 2.2.1. Fractions collected were analyzed by the developed HPLC method

Table 1
(a) Degradation rate constant (K_{obs}) and half life ($t_{1/2}$) for ATV at different temperatures and (b) rates of degradation reaction of ATV at different concentrations.

Temperature (°C)	K_{obs} (h^{-1})	$t_{1/2}$
(a)		
50	0.0411	6.602
60	0.0988	3.016
70	0.1336	2.253
80	0.3018	0.997

Test	$[ATV]_0$[a] ($mol\,L^{-1}$)	$[NaOH]_0$[b] ($mol\,L^{-1}$)	v[c] ($mol\,L^{-1}\,min^{-1}$)
(b)			
1	4.359×10^{-4}	0.02	4.518×10^{-4}
2	8.718×10^{-4}	0.02	8.220×10^{-4}
3	4.359×10^{-4}	0.04	9.064×10^{-4}

[a] Initial ATV concentration.
[b] Initial NaOH concentration.
[c] Rate of reaction.

to ensure purity. Fractions of >95% were pooled together, concentrated in vacuo to remove acetonitrile. The aqueous solution of each impurity was lyophilized using freeze drier (Virtis advantage 2XL, SP Industries, Gardiner, NY, USA). The isolated impurities RS3, RS10 and R12 were obtained as white powders. The chromatographic purity of the isolated impurities determined by the proposed HPLC method (Section 2.2.5) was found to be more than 95%. The degradation products RS8 and RS9 were isolated from the alkaline degradation of ATV. Based on the information from kinetic investigation of alkaline degradation, A 25 ml of ATV 5 mg/ml in 1:1 v/v mixture of water and ACN was treated with 25 ml of 0.02 M NaOH at 70 °C for 3 h to form about 50% of products. These degradation products were isolated by the preparative HPLC conditions described in Section 2.2.1. The fractions of the degradation products RS8 and RS9 were collected separately until the enrichment of products has become more than 90% and concentrated in vacuo to remove acetonitrile. The aqueous solutions were lyophilized using freeze drier. The purities of these isolated degradation products were determined chromatographically by the proposed HPLC method (Section 2.2.5) and they were found to be more than 98% for both the compounds. From the spectroscopic analysis of these isolated compounds by ESI-MS/MS, ^{1}H NMR, and FT-IR, the impurities are characterized. The ^{1}H NMR chemical shift data and FT-IR spectral data of ATV and the unknown impurities are presented in Tables 2 and 3

respectively. The MS/MS fragmentation patterns are shown in Fig. 3

2.6. Method validation

Validation of the chromatographic method was carried-out with regard to linearity, sensitivity (limit of detection, lod and limit of quantification, loq), precision, accuracy and robustness.

2.6.1. Linearity, LOD and LOQ

The linearity of detector response to different concentrations was evaluated for ATV and all the impurities using ten levels ranging from 0.020 μg/ml to 3.00 μg/ml equivalent to 0.002 (% w/w) to 0.300 (% w/w) with respect to sample concentration. The linear regression data for all the impurities tested were evaluated.

The LOD and LOQ were determined for ATV and each of the impurities based on the standard deviation of (SD) of the response and slope (S) of the regression line as per ICH guideline [27] accord-

Table 2
Comparative ^{1}H NMR assignments for ATV and its impurities (in DMSO-d_6).

Position[a]	Atazanavir		RS3		RS8		RS9		RS10		Position[a]	RS12	
	^{1}H	ppm/J_{Hz}	^{1}H	ppm/J_{Hz}	^{1}H	ppm/J_{Hz}	^{1}H	ppm/J_{Hz}	^{1}H	ppm/J_{Hz}		^{1}H	ppm/J_{Hz}
1	9H	0.76/s	9H	0.82/s	9H	0.80/s	9H	0.78/s	9H	1.24/s	1,1′	18H	0.62 and 0.76/4s
2	3H	3.52/s	3H	3.54/s	3H	3.53/s	3H	–	3H	3.51/s	2,2′	6H	3.52/2s
3	1H	6.87/d, 9.00	1H	6.83/d, 9.30	1H	6.84/d, 9.00	1H	6.83/d, 9.30	1H	6.86/d, 9.00	3,3′	2H	6.87/2d, 9.00, 9.00
4	1H	3.84/d, 9.60	1H	3.87/d, 9.80	1H	3.85/d, 9.30	1H	3.85/d, 9.00	1H	3.90/d, 9.60	4,4′	2H	3.84/2d, 9.60, 9.60
5	1H	7.54/d, 9.00	1H	7.57/d 8.50	1H	7.57/d, 7.40	1H	7.57/d, 7.90	1H	7.57/d, 9.00	5,5′	2H	7.54/2d, 9.00, 9.00
6	1H	4.04/m	1H	4.05/m	1H	4.21/m	1H	4.21/m	1H	4.10/m	6,6′	2H	4.04/2m
7	2H	2.77/m	2H	2.66 and 2.81/m	2H	2.77/m	2H	2.75/m	2H	2.67/m	7,7′	4H	2.77/2m
8	5H	7.13–7.20/m	5H	7.13–7.21/m	5H	7.15–7.22/m	5H	7.14–7.23/m	5H	7.14–7.21/m	8,8′	10H	7.13–7.20/2m
9	1H	3.59/m	1H	3.82/m	1H	3.53/m	1H	3.53/m	1H	3.52/m	9,9′	2H	3.59/2m
10	1H	5.02/s	1H	5.46/s	1H	4.80/s	1H	4.80/s	1H	4.67/s	10,10′	2H	5.02/2s
11	2H	2.79/m	2H	2.42/m,	2H	3.00/m	2H	3.02/m	2H	2.85/m	11,11′	4H	2.79/2m
12	1H	9.11/s	1H	–	1H	–	1H	–	1H	–	12,12′	2H	9.11/2s
13	2H	3.96/s	2H	3.62 and 3.69/ABq	2H	4.31/s	2H	4.35/s	2H	3.90/s	13,13′	4H	3.96/2s
14	2H	7.42/d, 7.90	2H	7.39/d, 8.2	2H	7.44/d, 7.90	2H	7.43/d, 7.80	2H	7.42/d, 8.20	14,14′	4H	7.42/2d, 7.90, 7.90
15	2H	7.97/d, 8.20	2H	8.02/d, 8.2	2H	7.96/d, 7.90	2H	7.96/d, 7.90	2H	7.97/d, 8.00	15,15′	4H	7.97/2d, 8.20, 8.20
16	2H	7.83–7.92/m	2H	7.87–7.95/m,	2H	7.85–7.92/m	2H	7.86–7.89/m	2H	7.86–7.93/m	16,16′	4H	7.83–7.92/2m
17	1H	7.33/dd	1H	7.34/dd	1H	7.33/dd	1H	7.34/dd	1H	7.33/dd	17,17′	2H	7.33/2dd
18	1H	8.65/d, 3.80	1H	8.66/d, 4.00	1H	8.64/d, 3.50	1H	8.64/d, 3.50	1H	8.64/d, 4.30	18,18′	2H	8.65/2d, 3.80
19	1H	3.64/d, 9.60	–	–	1H	3.63/d, 9.30	1H	3.61/d, 9.00	–	–	–	–	–
20	9H	0.62/s	–	–	9H	0.53/s	9H	0.57/s	9H	0.57/m	–	–	–
21	1H	6.98/d, 9.00	–	–	1H	8.14/s	1H	8.18/s	–	–	–	–	–
22	3H	3.52/s	–	–	–	–	3H	3.53/s	–	–	–	–	–

[a] Refer to Fig. 1 for numbering. s, singlet; d, doublet; dd, doublet of doublet; m, multiplet; ABq, AB quartet.

Table 3
FT-IR spectral data of ATV and its impurities.

Compound	IR (KBr) absorption bands (cm^{-1})
RS3	3332 NH and OH stretch, 3062, 3029 aromatic CH stretch, 2956 aliphatic CH stretch, 1717, 1657 C=O stretch, 1588 C=C stretch, 1515 aromatic C=C stretch, 1468, 1436, 1368 aliphatic CH bend, 1243 C–N stretch, 1066 C–O–C stretch, 779, 751 aryl CH out of plane bend.
ATV	3358, 3315 NH and OH stretch, 3061 aromatic CH stretch, 2964, 2909, 2875 aliphatic CH stretch, 1700, 1676, 1652 C=O stretch, 1626, 1531 aromatic C=C stretch, 1454, 1370 aliphatic CH bend, 1243 C–N stretch, 1067 C–O–C stretch, 777, 767 aryl CH out of plane bend.
RS8	3316 NH and OH stretch, 3061, 3029 aromatic CH stretch, 2962, 2872 aliphatic CH stretch, 1720, 1663, C=O stretch, 1559, 1517 aromatic C=C stretch, 1468, 1436, 1369 aliphatic CH bend, 1242 C–N stretch, 1069 C–O–C stretch, 781, 758 aryl CH out of plane bend.
RS9	3312 NH and OH stretch, 3029 aromatic CH stretch, 2962, 2872 aliphatic CH stretch, 1719, 1663 C=O stretch, 1559, 1517 aromatic C=C stretch, 1468, 1436, 1384, 1369 aliphatic CH bend, 1255 C–N stretch, 1069 C–O–C stretch, 781, 758 aryl CH out of plane bend.
RS10	3328 NH and OH stretch, 3062, 3029 aromatic CH stretch, 2968, 2873 aliphatic CH stretch, 1716, 1660 C=O stretch, 1589 C=C stretch, 1514 aromatic C=C stretch, 1468, 1456, 1437, 1368 aliphatic CH bend, 1250 C–N stretch, 1066 C–O–C stretch, 781, 749 aryl CH out of plane bend.
RS12	3324 NH and OH stretch, 3085, 3062, 3029 aromatic CH stretch, 2959, 2872, aliphatic CH stretch, 1712, 1661 C=O stretch, 1588, 1515 aromatic C=C stretch, 1468, 1455, 1436, 1398, 1368 aliphatic CH bend, 1242 C–N stretch, 1066 C–O–C stretch, 779, 749 aryl CH out of plane bend.

ing to the formulas give below.

$$\mathrm{LOD} = \frac{3.3 \times \mathrm{SD}}{S} \quad (1)$$

$$\mathrm{LOQ} = \frac{10 \times \mathrm{SD}}{S} \quad (2)$$

The residual sum of squares obtained from linearity regression data is used as SD.

2.6.2. Precision

The precision in determining the ATV impurities was studied by repeatability (system and method precision) and intermediate precision (ruggedness). ATV solution of 0.2% w/w was injected for six times to evaluate the precision of the system. Precision of the method was studied for repeatability and intermediate precision. Repeatability was demonstrated by analyzing six separate ATV sample solutions spiked with all the impurities at specification level. The intermediate precision of the method was determined on six separate sample solutions prepared from same lot by spiking the impurities at specification level by a different analyst using different instrument with different lot of column for 2 days.

2.6.3. Accuracy

Accuracy of the method by recoveries of all the impurities was determined by analyzing ATV sample solutions spiked with each impurity at four different concentration levels ranging from LOQ to 150% in triplicate with respect to specified limit.

2.6.4. Robustness

The robustness of the method was evaluated through the studies of influence of small and premeditated alteration of analytical parameters. The parameters selected were flow rate (±10%), mobile phase composition (±2% of gradient composition), column temperature (±5 °C) and pH of buffer (±0.2 unit). Only one parameter was altered while the remaining parameters were kept constant. Solutions of ATV spiked with impurities at each of the above varied parameters were analyzed on Waters HPLC (low pressure, dwell volume 0.6 ml). Further, the robustness of the method in the above mentioned variations are studied using two more brands of HPLCs (Agilent HPLC/low pressure, dwell volume 1 ml and Shimadzu HPLC/high pressure, dwell volume 3 ml) to find if dwell volume has any influence on the separation of the impurities.

2.6.4.1. Stability of analytical solution. To determine the stability of sample solution, the sample solution of ATV spiked with impurities at specified level was subjected to analysis immediately after preparation and regularly after 1 h time interval up to 24 h, while maintaining the sample cooler temperature at 25 °C.

3. Results and discussion

The structures of ATV, its process impurities (RS1–RS7 and RS10–RS13) and degradants (RS8 and RS9) are depicted in Fig. 1. The compounds RS1 and RS13 are process intermediates. RS2, RS3, RS4, RS5, RS6, RS7, RS10, RS11 and RS12 are process impurities produced during the synthesis of ATV [28] as depicted in Fig. 4. The origin of impurities is provided in Table 4. The present study was aimed at developing a liquid chromatographic method for the separation and quantitative determination of ATV impurities. It may be noted that the process intermediate N-methoxycarbonyl-L-tert-leucine is monitored by a separate HPLC method as it is relatively more polar, elutes in void time and is not detected due to limited UV chromophoric activity at 250 nm. Further, studies were carried out to characterize the unknown impurities of ATV.

3.1. Structural elucidation of process impurities and degradation products

3.1.1. Structure elucidation of RS3

The impurity RS3 exhibited a protonated molecular ion peak at *m*/*z* 534 in positive ion ESI-MS analysis and the difference of mass between ATV and RS3 was 171 amu, indicating the absence of N-(methoxycarbonyl)-tert-leucine moiety on either side of ATV. The impurity RS3 and ATV are subjected to ESI-MS/MS analysis and the fragmentation pattern of RS3 is different from that of ATV (Fig. 3a and b). The major product ions of ATV are observed at *m*/*z* 687, 612, 534, 335, 168 and 144 and of RS3 are at *m*/*z* 363, 335, 168 and 144 (Fig. 3) resembling the probable fragmentation pattern of RS3. The ^{1}H NMR and FT-IR spectral data of ATV and all unknown impurities are given in Tables 2 and 3 respectively. ^{1}H NMR spectral data of RS3 showed chemical shift similarity with ATV except the signal at 0.80 ppm corresponding to 9 protons instead of 18 protons (at 0.62 ppm and 0.76 ppm) and a small up field shift observed for two –NCH_2 signals from 2.79 ppm, 3.96 ppm to 2.42 ppm, and 3.62 and 3.69 ppm respectively, while the signals corresponding to N-(methoxycarbonyl)-tert-leucine at 3.64 ppm, 6.98 ppm and 3.52 ppm in comparison with ATV were absent. From this spectral information the structures is confirmed as (3S,6S,7S)-9-amino-3-(1,1-dimethylethyl)-7-hydroxy-4-oxo-6-(phenylmethyl)-10-[-4-(2-pyridinyl) phenyl]-2,5,9,-triazadecanoic acid methyl ester.

Table 4
Origin and classification of ATV impurities.

Compound	Origin	Classification
RS1	In the preparation of atazanavir base, diamino hydrochloride intermediate (RS1) which is prepared from DIBOC intermediate (RS13) is condensed in situ with N-methoxycarbonyl-L-tert-leucine (MOC-L-tert-leucine). During this condensation unreacted RS1 gets carried to atazanavir.	P
RS2	RS13 may contain pyridyl benzylhydrazine as an impurity. This impurity can undergo sequence of reactions along with RS13 and lead to hydrazine leucine impurity (RS2) in atazanavir base.	P
RS3	The formation of atazanavir base takes place through monoacyl atazanavir amine intermediate (RS3), when RS1 is condensed with MOC-L-tert-leucine. During this condensation incompletely converted RS1 gets carried to atazanavir. RS3 can also result from the hydrolytic degradation of atazanavir.	P/D
RS4	4-(Pyridine-2-yl)benzaldehyde which is used as starting material in the preparation of RS13, may contain the positional isomer, 4-(pyridine-4-yl)benzaldehyde as an impurity. This impurity undergoes the sequence of reactions during the preparation of atazanavir and results in 4-pyridyl atazanavir impurity (RS4) in atazanavir.	P
RS5	2(R)–[(1′S)-(tert-Butyloxycarbonyl)amino-2′-phenylethyl]oxirane which is used as intermediate in the preparation of RS13, may contain 2(S)–[(1′S)-(tert-butyloxycarbonyl)amino-2′-phenylethyl]oxirane as an impurity. This impurity undergoes the sequence of reactions during the preparation of atazanavir and results in SRSS-atazanavir diastereomer impurity (RS5) in atazanavir.	P
RS6	SSRS-atazanavir diastereomer (RS6) is formed during the preparation of atazanavir from MOC-L-tert-leucine and RS13.	P
RS7	(D)-tert-Leucine, an impurity of (L)-tert-leucine which is used in the preparation of the atazanavir intermediate MOC-L-tert-leucine undergoes reaction sequence resulting in RSSR-atazanavir diastereomer impurity (RS7) in atazanavir.	P
RS8 and RS9	When atazanavir subjected to alkaline hydrolysis in presence of heat, MOC-L-tert-leucine moieties present on either side of atazanavir molecule under goes cyclization with the elimination of methanol leading to base cyclization products RS8 (due to right-side cyclization) and RS9 (left-side cyclization)	D
RS10	The formation of RS1 takes place through BOC monoacyl atazanavir (RS10), when the BOC groups of RS13 are deprotected by treating with concentrated hydrochloric acid. The incompletely deprotected RS13 further undergoes reaction sequence of atazanavir leading to RS10 in atazanavir.	P
RS11	MOC-L-tert-leucine is prepared by acylation of L-tert-leucine with methyl chloroformate. This methyl chloroformate may contain ethyl chloroformate as an impurity, thus resulting N-(ethoxycarbonyl)-(L)-tert-leucine in MOC-L-tert-leucine. This impurity undergoes condensation with RS1 resulting in ECF atazanavir (RS11) in atazanavir base.	P
RS12	The RS3 formed during the preparation of atazanavir base may further condense with methoxycarbonyl function of MOC-L-tert-leucine resulting in monoacyl atazanavir dimer impurity (RS12). This can also form via the condensation of RS3 with MOC-L-tert-leucine which are produced from the hydrolytic degradation of atazanavir.	P/D
RS13	RS13 is used in the preparation of RS1, the unreacted RS13 which remains as an impurity in RS1 gets carried to final atazanavir.	P

3.1.2. Structure elucidation of RS8 and RS9

In the positive mode ESI-MS analysis of the impurities RS8 and RS9 exhibited a protonated molecular ion peak of same *m*/*z* 673 indicating isomeric nature of these two impurities. The difference of mass between ATV and each impurity is 32 amu, indicating the absence of $–OCH_3$ group of right and left side moiety corresponding to ATV is observed in RS8 and RS9 respectively. The major product ions observed from ESI-MS/MS analysis of RS8 and RS9 (Fig. 3c and d) at *m*/*z* 655, 502, 168 and 144 are common for both the impurities while the fragment ion at *m*/*z* 335 is observed only for RS8. Structural interpretation has been explained in Table 2. These two isomeric impurities of dioxoimidazolidine moiety are formed through internal cyclization between two amide –NH protons either at right side or left side moiety of L-tert leucine with respect to ATV. In ^{1}H NMR the absence of one amide –NH proton either right side or left side moiety of RS8 and RS9 confirms the formation of dioxoimidazolidine moiety. From this spectral information the structures of RS8 and RS9 are confirmed as (3S,6S,7S)-3-(1,1-dimethylethyl)-7-hydroxy-4-oxo-6-(phenylmethyl)-9-[[4-(2-pyridinyl) phenyl]methyl]-9-[4-(1,1-dimethylethyl)-2,5-dioxoimidazolidin-1-yl)]-2,5,9-triiaznonoic acid methyl ester; and (3S,8S,9S)-3-(1,1-dimethylethyl)-8-hydroxy-4-oxo-9-(phenylmethyl)-6-[[4-(2-pyridinyl) phenyl]methyl]-9-[4-(1,1-dimethylethyl)-2,5-dioxoimidazolidin-1-yl)]-2,5,6-triiazaonoic acid methyl ester respectively (Fig. 5).

3.1.3. Structure elucidation of RS10

The impurity RS10 exhibited a protonated molecular ion peak at *m*/*z* 634 in positive ion ESI-MS analysis and the difference of mass between ATV and impurity was 71 amu, indicating methoxy carbonyl moiety either in right side or left side of ATV. The major product ions observed from ESI-MS/MS analysis of RS10 (Fig. 3e) were at *m*/*z* 578, 534, 335 and 168. The ^{1}H NMR spectral data of RS10 (Table 2) showed similarity in chemical shift values in comparison with ATV except the signals at 3.64 ppm, 6.98 ppm and 3.52 ppm were absent. But, in ^{1}H NMR a comparative downfield shift observed for tert-butyl protons either right side or left side moiety from 0.76 ppm to 1.24 ppm indicates possibility of attachment of tert-butyl group with the oxygen atom instead of methine carbon. From the above spectral information and the possibility of occurrence of this impurity from the synthesis of ATV, the structure was confirmed as (3S,6S,7S)-3-(1,1-dimethylethyl)-7-hydroxy-4-oxo-6-(phenylmethyl)-9-[[4-(2-pyridinyl)phenyl]methyl]-9-[(tert-butyloxycarbonyl)amino]-2,5,9,-triazanonoic acid methyl ester.

3.1.4. Structure elucidation of RS12

The impurity RS12 exhibited a protonated molecular ion peak at *m*/*z* 1094 in positive ion ESI-MS analysis and the difference of mass between ATV and impurity was 389 amu indicating a dimeric compound. The ESI-MS/MS fragmentation pattern (Fig. 3f) of the impurity was different from that of ATV. The major

Table 5
Selectivity of C8 columns of different manufacturer in the optimized chromatographic conditions.

Column	Compound	*k*	*α*	Rs	*T*
Symmetry C8, 250 mm × 4.6 mm, 3 μm	RS1	0.7	6.12	–	2.2
	RS2	4.0	1.12	12.1	1.0
	RS3	4.5	2.03	2.9	0.9
	RS4	9.1	1.35	25.0	1.2
	RS5	12.2	1.08	12.3	0.9
	ATV	13.2	1.07	3.5	0.8
	RS6	14.2	1.06	3.4	0.9
	RS7	15.0	1.03	2.9	0.9
	RS8	15.6	1.03	1.8	0.9
	RS9	16.0	1.12	1.6	0.9
	RS10	17.9	1.05	6.1	0.9
	RS11	18.8	1.05	2.5	0.9
	RS12	19.6	1.21	2.5	0.9
	RS13	23.8	–	14.7	0.9
YMC Pack C8, 150 mm × 4.6 mm, 3 μm	RS1	0.6	5.59	–	1.7
	RS2	3.4	1.18	15.5	1.1
	RS3	4.0	2.09	4.5	1.0
	RS4	8.4	1.24	26.7	1.0
	RS5	10.5	1.08	9.3	1.1
	ATV	11.3	1.07	3.9	0.9
	RS6	12.1	1.06	3.6	1.0
	RS7	12.8	1.05	3.1	1.1
	RS8	13.4	1.03	2.7	1.0
	RS9	13.8	1.12	1.8	1.0
	RS10	15.5	1.04	6.8	0.9
	RS11	16.0	1.05	2.3	1.0
	RS12	16.8	1.24	3.3	0.9
	RS13	20.8	–	17.5	1.0
Ascentis® Express, 150 mm × 4.6 mm, 2.7 μm	RS1	0.5	6.04	–	1.3
	RS2	3.2	1.26	17.4	1.2
	RS3	4.1	2.02	6.2	1.2
	RS4	8.3	1.37	34.5	1.0
	RS5	11.4	1.09	18.4	1.1
	ATV	12.5	1.08	4.9	0.9
	RS6	13.4	1.06	4.8	1.0
	RS7	14.2	1.04	3.8	1.0
	RS8	14.7	1.03	2.5	1.0
	RS9	15.2	1.13	2.1	1.0
	RS10	17.2	1.06	8.6	1.1
	RS11	18.2	1.06	4.7	1.0
	RS12	19.2	1.26	4.7	0.9
	RS13	24.2	–	23.1	1.0
Hypersil BDS C8, 150 mm × 4.6 mm, 3 μm	RS1	0.8	2.99	–	1.4
	RS2	2.5	1.75	9.5	1.2
	RS3	4.3	1.52	10.3	0.9
	RS4	6.6	1.24	11.6	1.1
	RS5	8.1	1.07	6.6	1.1
	ATV	8.7	1.08	2.2	1.1
	RS6	9.4	1.07	2.6	1.1
	RS7	10.1	1.02	2.7	0.8
	RS8	10.4	1.03	1.1	1.2
	RS9	10.7	1.12	1.3	1.4
	RS10	12.0	1.05	4.3	1.0
	RS11	12.5	1.11	1.7	1.1
	RS12	13.9	1.23	4.3	1.1
	RS13	17.1	–	9.4	1.1

k, retention factor; *α*, selectivity; Rs, resolution; *T*, tailing factor.

product ions observed were at *m*/*z* 760, 560, 534, 335, 168 and 144. In ^{1}H NMR, the chemical shifts of all the signals of RS12 show similarity with ATV except signals corresponding to the N-(methoxycarbonyl)-tert-leucine moiety. The additional aromatic proton signals corresponded to double the number of aromatic protons with respect to ATV suggests the dimeric structure. All the NMR signal chemical shift values of this impurity resemble with RS3 with double the number of aromatic protons (26 protons) indicating dimerization of RS3 by the loss of water molecule at amino moiety. The three singlet signals at 6.56 ppm, 6.71 ppm, 7.53 ppm of 6 protons which are exchangeable with D_2O indicates 6 amide protons of two molecules of RS3 get condensed. From this spectral information the structure was confirmed as 1,3-Bis-[3(S)-(dimethylethyl)-7(S)-hydroxy-4-oxo-6(S)-(phenylmethyl)-9-[[4-(2-pyridinyl)phenyl]methyl]-2,5,9,-triazanonoic acid methyl ester-9-yl] urea (Fig. 5).

3.2. Optimization of HPLC conditions

In preliminary experiments ATV and all the impurities were subjected to separation by RP-HPLC method described by Seshachalam et al. [13]. The retention factors (*k*) of all these impurities were found to be in between 0.1 and 24. The peaks due to compounds ATV, RS6, RS10, RS11, RS12, and RS13 did not separate and RS7, RS8

Table 6
Linearity, LOD and LOQ data for ATV and its impurities.

Compound	Calibration range (μg/ml)	Regression equation	SES[a]	SEI[b]	CC[c] (r)	δ[d]	CF[e]	LOD (μg/ml) (% RSD)	LOQ (μg/ml) (% RSD)
RS1	0.020–3.012	$y = 29607x - 18$	82 (±189)	125 (±288)	0.9998	661	0.82	0.074 (5.5)	0.223 (0.9)
RS2	0.020–2.989	$y = 35359x - 254$	423 (±975)	640 (±1476)	0.9997	882	0.68	0.082 (6.2)	0.223 (1.5)
RS3	0.021–3.083	$y = 29963x - 492$	156 (±360)	243 (±560)	0.9997	791	0.81	0.087 (7.6)	0.264 (2.2)
RS4	0.020–2.997	$y = 16313x + 109$	141 (±325)	213 (±491)	0.9997	429	1.48	0.087 (7.8)	0.263 (3.2)
RS5	0.020–3.019	$y = 23200x + 10$	190 (±438)	289 (±666)	0.9997	569	1.04	0.081 (9.2)	0.245 (4.0)
ATV	0.020–3.005	$y = 24142x - 13$	143 (±330)	217 (±500)	0.9997	563	1.00	0.077 (8.2)	0.233 (3.3)
RS6	0.020–3.068	$y = 25060x - 122$	326 (±752)	506 (±1167)	0.9996	531	0.96	0.070 (7.1)	0.212 (2.8)
RS7	0.020–3.054	$y = 23810x - 18$	127 (±293)	195 (±450)	0.9997	586	1.01	0.081 (7.0)	0.246 (2.8)
RS8	0.020–3.012	$y = 19683x - 261$	108 (±249)	165 (±380)	0.9997	528	1.23	0.089 (6.8)	0.263 (2.8)
RS9	0.020–3.060	$y = 19551x - 251$	79 (±182)	122 (±281)	0.9997	532	1.23	0.090 (9.5)	0.272 (3.6)
RS10	0.020–3.042	$y = 24512x + 132$	55 (±127)	85 (±196)	0.9998	524	0.98	0.074 (9.1)	0.214 (3.2)
RS11	0.020–3.057	$y = 23100x - 74$	250 (±577)	385 (±888)	0.9997	564	1.05	0.081 (8.8)	0.244 (3.2)
RS12	0.020–3.043	$y = 28110x - 102$	119 (±274)	183 (±422)	0.9997	672	0.86	0.079 (8.4)	0.239 (3.2)
RS13	0.019–2.913	$y = 29523x - 164$	274 (±632)	402 (±927)	0.9998	570	0.82	0.064 (6.4)	0.193 (3.2)

[a] Standard error of slope and the values given in parentheses are 95% confidence limits.
[b] Standard error of intercept and the values given in parentheses are 95% confidence limits.
[c] Correlation coefficient.
[d] Standard deviation of peak areas (residual standard deviation of y on x).
[e] Correction factor.

and RS9 were poorly separated in this condition. The attempts to improve selectivity, peak shapes and to reduce the retention times by altering buffer pH, acetonitrile/methanol in different combinations were not successful.

So, further separation experiments were carried out by RP-HPLC on C8 columns of different manufacturers which are equivalent in dimensions and stationary phase, (i) Symmetry C8, 150 mm × 4.6 mm, 3 μm; (ii) YMC Pack C8, 150 mm × 4.6 mm, 3 μm; (iii) Ascentis® Express C8, 150 mm × 4.6 mm 2.7 μm; and (iv) Hypersil BDS C8, 150 mm × 4.6 mm, 3 μm using mobile phase of H_2O/ACN and H_2O/methanol in different compositions. Broad peak shapes and asymmetry were observed for ATV and its impurities. To improve this and due to varying polarities of the compounds, further trials were conducted with KH_2PO_4 (0.02 M) buffer and methanol/ACN in gradient mode with different time programs. With ACN, comparatively sharp peaks and good resolution were obtained relative to methanol. On further optimization of the gradient composition using ACN as organic modifier, optimal separation was achieved with gradient program as given in Section 2.2.5. The column selectivity [29] for the separation of impurities was explored on these columns and data presented in Table 5, which showed the compounds were well separated with good peak shapes on Ascentis column. The superior separation efficiency of Ascentis column could be ascribed to sub-3μ particle size resulting from smaller plate heights compared to 3μ particle size of other columns. So it was preferred for further optimization on the effect of concentration and pH of buffer on the separation of ATV and its impurities. YMC Pack C8 column may be chosen as an alternative column.

The study of the effect of concentration of KH_2PO_4 on the separation and retention was studied by varying its concentration from 0.01 to 0.03 M. Buffer concentration showed no effect on the retention and resolution. So 0.02 M KH_2PO_4 was selected as buffer and studied by adjusting to different pHs with OPA. The pH showed no effect on the retention times of the compounds (RS1, RS3), while retention of remaining compounds was slightly increased with increase in buffer pH. At pH 2.5, (RS4, RS5) co-eluted and (RS8, RS9) eluted closely. At pH 3.0, the resolution between (RS4, RS5) increased significantly, while RS6 eluted closely to ATV and (RS8, RS9) separated well. At pH 4.5, 5.5 and 6.5, the peaks due to (RS2, RS3) co-eluted, where as the resolution of the pair (RS4, RS5) decreased. The peaks due to (RS8, RS9) eluted very closely in the conditions of pH 2.5 and 3.5; and they co-eluted at pH 6.5. However, at pH 3.5, all the related substances were separated. The UV spectra of ATV and its impurities showed absorption maxima at 250 nm and 280 nm; at 250 nm optimal response for all the compounds has been obtained. So finally separation was carried out on Ascentis® express C8 column maintained at 30 °C with gradient elution using KH_2PO_4 (pH 3.5, 0.02 M) as buffer and ACN as organic modifier with PDA detector set at 250 nm as the wavelength of detection. A typical chromatogram of ATV spiked with impurities at 0.2% w/w is shown in Fig. 6.

3.3. Results of forced degradation

When ATV was subjected to solution state forced degradation (acid, alkaline and peroxide) the drug molecule degraded up to 2% in acid hydrolytic condition resulting two unknown impurities at RRT-0.78(2.91%) and 0.85(0.68%) along with the small level of RS3 (0.09%). The alkaline degradation resulted in 8% of two unknown impurities at RRT-1.17(4.94%) and 1.21(3.08%) while in the oxidative stress of the drug molecule few unknown impurities formed which are in the range of 0.07–0.40%. Whereas under solid state forced degradations ATV did not degrade. The unknown degradants produced in the forced degradation are separated well (Rs > 2.5) from ATV and known impurities. The two degradation products of alkaline condition are isolated and characterized as RS8 and RS9. The peak homogeneity of impurities and ATV was verified using Waters Empower Software and found to be pure (purity angle is less than purity threshold). The pathways of ATV degradation under alkaline condition is presented in Fig. 5.

3.3.1. Kinetics of alkaline degradation

The degradation of ATV under alkaline condition at the selected temperatures (40, 50, 60, and 80 °C) followed first order kinetics and the results of rate constant and half life time of the degradation process are given in Table 1a. And also the reaction rates were measured as per the method of initial rates by varying the concentration of ATV at constant concentration of NaOH as shown in tests 1 and 2 (Table 1) and the order of reaction with respect to ATV was determined as followed.

$$\frac{4.518 \times 10^{-4}}{8.220 \times 10^{-4}} = \frac{k[4.359 \times 10^{-4}]^a \times [0.02]^b}{k[8.718 \times 10^{-4}]^a \times [0.02]^b}$$

$$0.5596 = [0.5]^a$$

On solving the above equation, a was found equivalent to 1, so order of reaction with respect to ATV is one. Likewise reaction rates were measured by varying concentration of NaOH and keeping the concentration of ATV constant as shown in tests 2 and 3 (Table 1)

Table 7
Accuracy data of ATV impurities.

Compound	50% of specification level[a]			100% of specification level[a]			150% of specification level[a]			LOQ level		
	Amount (% w/w)			Amount (% w/w)			Amount (% w/w)			Amount (% w/w)		
	Added[b]	Found[b]	% Recovery[c]	Added[b]	Found[b]	% Recovery[c]	Added[b]	Found[b]	% Recovery[c]	Added[b]	Found[b]	% Recovery[c]
RS1	0.100	0.104	103.7 ± 0.6	0.201	0.200	99.7 ± 0.3	0.301	0.299	99.3 ± 0.4	0.0223	0.0220	98.7 ± 0.9
RS2	0.099	0.100	100.7 ± 0.6	0.198	0.198	100.0 ± 0.5	0.296	0.297	100.7 ± 0.1	0.0247	0.0243	98.4 ± 1.8
RS3	0.100	0.099	99.3 ± 0.6	0.200	0.199	99.3 ± 0.8	0.300	0.298	99.3 ± 0.4	0.0212	0.0203	95.8 ± 0.5
RS4	0.100	0.101	101.3 ± 1.5	0.199	0.202	101.5 ± 0.5	0.299	0.300	100.5 ± 0.7	0.0270	0.0263	97.6 ± 1.1
RS5	0.099	0.097	98.3 ± 0.6	0.198	0.200	100.7 ± 0.8	0.297	0.297	100.0 ± 0.3	0.0249	0.0243	97.7 ± 1.5
RS6	0.100	0.098	98.3 ± 0.6	0.200	0.199	99.7 ± 0.3	0.299	0.290	96.9 ± 0.4	0.0218	0.0224	102.8 ± 1.6
RS7	0.100	0.098	98.0 ± 1.0	0.200	0.202	100.8 ± 0.8	0.300	0.294	98.0 ± 0.3	0.0250	0.0245	98.3 ± 1.0
RS8	0.101	0.100	98.7 ± 0.6	0.201	0.202	100.3 ± 1.3	0.301	0.297	98.8 ± 0.9	0.0271	0.0274	101.3 ± 0.4
RS9	0.099	0.098	98.7 ± 0.6	0.199	0.199	100.0 ± 0.5	0.297	0.295	99.3 ± 0.4	0.0271	0.0265	97.8 ± 1.4
RS10	0.100	0.099	98.7 ± 1.2	0.199	0.199	99.8 ± 0.6	0.298	0.297	99.3 ± 0.9	0.0218	0.0213	97.7 ± 0.5
RS11	0.099	0.098	99.0 ± 1.0	0.199	0.197	99.0 ± 1.3	0.298	0.299	100.4 ± 0.2	0.0250	0.0249	99.7 ± 0.6
RS12	0.099	0.098	98.7 ± 0.6	0.199	0.195	98.0 ± 0.5	0.298	0.291	97.9 ± 0.8	0.0240	0.0238	99.1 ± 2.1
RS13	0.104	0.102	98.4 ± 0.5	0.207	0.208	100.3 ± 0.8	0.310	0.308	99.6 ± 0.4	0.0200	0.0197	98.5 ± 0.8

[a] Specification level 0.2% w/w for all the impurities.
[b] $n = 3$, average of three determinations.
[c] Average ± RSD.

and the order of reaction with respect to NaOH was determined as followed.

$$\frac{4.518 \times 10^{-4}}{9.064 \times 10^{-4}} = \frac{k[4.359 \times 10^{-4}]^a \times [0.02]^b}{k[4.359 \times 10^{-4}]^a \times [0.04]^b}$$
$$0.4984 = [0.5]^b$$

On solving the above equation, a was found equivalent to 1, so order of reaction with respect to NaOH is one. So, the overall order of alkaline degradation reaction of ATV is two.

3.4. Method validation

3.4.1. System suitability test

The solution of ATV (1140 μg/ml) spiked with 0.2% w/w of impurities was analyzed during validation studies. From the data collected for RRTs, Resolutions between successive pairs and tailing factors of the compounds for all the validation experiments, it is found that the resolution value of more than 2.0 was achieved for all the pair of compounds and no significant variation in the RRTs and tailing factors of the compounds. Based on the minimum and maximum resolution achieved between the critical pairs (RS7, RS8) and (RS8, RS9), a resolution of not less than 2.2 and 2.0 were respectively set as system suitability requirement (the results are provided in Table S1 as supplementary data).

3.4.2. Linearity, LOD and LOQ

The linear regression results (Table 6) indicated the detector response at 250 nm were linear over the concentration range studied. The CF for each impurity was calculated against ATV, as the ratio of slope of ATV to slope of given impurity obtained from the regression line.

The concentrations of LODs and LOQs for ATV and its impurities were found to be in the range of 0.064–0.090 μg/ml and 0.193–0.272 μg/ml respectively. The concentrations of LODs and LOQs were verified for precision by the analysis of solutions having ATV and its impurities at these levels in six replicates and found to be below 10% RSD (Table 6).

3.4.3. Precision

The system precision evaluated using ATV solution of 0.2% w/w was 0.7%. The RSD values obtained for method precision were in the range of 0.5–2.5% ($n = 6$), indicated good repeatability. The intermediate precision of the method was determined as overall RSD and found to be below 3.0% for all the impurities.

3.4.4. Accuracy

The recoveries and RSDs of all these impurities were found to be in between 95.8–103.7% and 0.5–2.5% respectively (Table 7).

3.4.5. Robustness

The % difference for each impurity was evaluated and found to be in between 1.2% and 4.8% from the robustness studies involving deliberate changes in flow rate (±10%), mobile phase composition (±2% of gradient composition), column temperature (±5 °C) and pH of buffer (±0.2 unit). The studies indicated no effect on the determination of related substances and selectivity for the stability indicating test method is sufficiently robust to carry the quantification of impurities in quality assurance of ATV. Further the method's capability to remain unaffected with the different makes of HPLCs/dwell volumes also studied. The results showed the different dwell volumes of HPLC systems did not affect the resolution and selectivity except the resolution between RS7 and RS8 decreased to below 2.0 (1.5–1.8, as obtained for all the variations) from the test method value of 2.5 with waters HPLC. With other two systems the resolutions are more than 2.0 at all the varied conditions suggesting that the stability indicating test method is sufficiently robust to carry the quantification of impurities in quality assurance

Table 8
Results of analysis of ATV for impurities.

Batch	Impurity, mean[a] (% w/w)/% RSD												
	RS1	RS2	RS3	RS4	RS5	RS6	RS7	RS8	RS9	RS10	RS11	RS12	RS13
# 01	ND	ND	0.04	ND	BLQ	ND	ND	ND	ND	0.07	ND	BLQ	0.04
# 02	ND	ND	0.03	ND	BLQ	ND	ND	ND	ND	0.06	ND	BLQ	0.03
# 03	ND	ND	0.05	ND	BLQ	ND	ND	ND	ND	0.06	ND	BLQ	0.03

ND: not detected.
BLQ: below limit of quantitation.
[a] Mean of three determinations.

of ATV. The resolution and selectivity data obtained from the analysis of impurities spiked ATV sample solution at each of the above varied conditions using the three different HPLCs is presented as supplementary data in Table S2.

3.4.5.1. Stability of analytical solution. The % difference in peak area of all the impurities from initial to relevant time interval was calculated and found to be below 5.0%. So, sample solution was declared to be stable for at least 24 h at room temperature.

3.4.6. Application of the method

Three batches of ATV drug substance each in triplicate are analyzed using the proposed method. The levels of impurities relative to ATV were in the range of 0.02–0.07%. As per European Pharmacopoeia [30], if the correction factors of the impurities lie between 0.8 and 1.2, correction factors need not be considered in the evaluation of impurity levels. Therefore, correction factors are required for RS2, RS4, RS8 and RS9 as their responses are outside the Ph.Eur. acceptable response range of 0.8–1.2. The RSD ($n = 3$) for the impurities detected in the samples was below 10.0% (Table 8).

4. Conclusions

A gradient RP-HPLC method was developed and validated for quantitative determination of impurities of ATV drug substance. The method has higher sensitivity towards the determination of impurities and is found to be specific, sensitive, precise, linear, accurate and robust. Five unknown impurities, which are not reported earlier, are identified by this method, isolated and characterized using spectral data. Thus, this method can be implemented for routine testing as well as stability analysis of ATV drug substance.

Acknowledgement

The authors wish to thank the management of Aurobindo Pharma Limited Research Center for their support, encouragement and permitting this work to communicate for publication.

Appendix A. Supplementary data

Supplementary data associated with this article can be found, in the online version, at doi:10.1016/j.jpba.2011.01.002.

References

[1] Physician's Desk Reference, 63rd edition, Thomson Reuters, NJ, USA, 2009, 3299–3310.
[2] R. ter Heine, M. Davids, H. Rosing, E.C.M. van Gorp, J.W. Mulder, Y.T. van der Heide, J.H. Beijnen, A.D.R. Huitema, Quantification of HIV protease inhibitors and non-nucleoside reverse transcriptase inhibitors in peripheral blood mononuclear cell lysate using liquid chromatography coupled with tandem mass spectrometry, J. Chromatogr. B 877 (2009) 575–580.
[3] R. ter Heine, H. Rosing, E.C.M. van Gorp, J.W. Mulder, W.A. van der Steeg, J.H. Beijnen, A.D.R. Huitema, Quantification of protease inhibitors and non-nucleoside reverse transcriptase inhibitors in dried blood spots by liquid chromatography–triple quadrupole mass spectrometry, J. Chromatogr. B 867 (2008) 205–212.
[4] A. D'Avolio, M. Siccardi, M. Sciandra, B. Lorena, S. Bonora, L. Trentini, G. Di Perri, HPLC–MS method for the simultaneous quantification of the new HIV protease inhibitor darunavir, and 11 other antiretroviral agents in plasma of HIV-infected patients, J. Chromatogr. B 859 (2007) 234–240.
[5] R. ter Heine, C.G. Alderden Los, H. Rosing, M.J.X. Hillebrand, E.C.M. van Gorp, A.D.R. Huitema, J.H. Beijnen, Fast and simultaneous determination of darunavir and eleven other antiretroviral drugs for therapeutic drug monitoring: method development and validation for the determination of all currently approved HIV protease inhibitors and non-nucleoside reverse transcriptase inhibitors in human plasma by liquid chromatography coupled with electrospray ionization tandem mass spectrometry, Rapid Commun. Mass Spectrom. 21 (2007) 2505–2514.
[6] L. Dickinson, L. Robinson, J. Tjia, S. Khoo, D. Back, Simultaneous determination of HIV protease inhibitors amprenavir, atazanavir, indinavir, lopinavir, nelfinavir, ritonavir, and saquinavir in human plasma by high-performance liquid chromatography–tandem mass spectrometry, J. Chromatogr. B 829 (2005) 82–90.
[7] T. Koal, H. Burhenne, R. Roemling, M. Svoboda, K. Resch, V. Kaever, Quantification of antiretroviral drugs in dried blood spot samples by means of liquid chromatography/tandem mass spectrometry, Rapid Commun. Mass Spectrom. 19 (2005) 2995–3001.
[8] S. Colombo, A. Beguin, A. Telenti, J. Biollaz, T. Buclin, B. Rochat, L.A. Decosterd, Intracellular measurements of anti-HIV drugs indinavir, amprenavir, saquinavir, ritonavir, nelfinavir, lopinavir, atazanavir, efavirenz and nevirapine in peripheral blood mononuclear cells by liquid chromatography coupled to tandem mass spectrometry, J. Chromatogr. B 819 (2005) 259–276.
[9] K.M.L. Crommentuyn, H. Rosing, M.J.X. Hillebrand, A.D.R. Huitema, J.H. Beijnen, Simultaneous quantification of the new HIV protease inhibitors atazanavir and tipranavir in human plasma by high-performance liquid chromatography coupled with electrospray ionization tandem mass spectrometry, J. Chromatogr. B 504 (2004) 359–367.
[10] M. Jemal, S. Rao, M. Gatz, D. Whigan, Liquid chromatography–tandem mass spectrometric quantitative determination of the HIV protease inhibitor atazanavir (BMS-232632) in human peripheral blood mononuclear cells (PBMC): practical approaches to PBMC preparation and PBMC assay design for high-throughput analysis, J. Chromatogr. B 795 (2003) 273–289.
[11] A. Schuster, S. Burzawa, M. Jemal, E. Loizillon, P. Couerbe, D. Whigan, Quantitative determination of the HIV protease inhibitor atazanavir (BMS-232632) in human plasma by liquid chromatography–tandem mass spectrometry following automated solid-phase extraction, J. Chromatogr. B 788 (2003) 377–386.
[12] D. Cattaneo, F. Maggiolo, D. Ripamonti, N. Perico, Determination of atazanavir in human plasma by high-performance liquid chromatography with UV detection, J. Chromatogr. Sci. 46 (2008) 485–489.
[13] U. Seshachalam, D.V.L. Narasimha Rao, B. Haribabu, K.B. Chandrasekhar, Determination of atazanavir in the presence of its degradation products by a stability-indicating LC method, Chromatographia 65 (2007) 355–358.
[14] K. Keil, J. Hochreitter, R. DiFrancesco, B.S. Zingman, R.C. Reichman, M.A. Fischl, B. Gripshover, G.D. Morse, Integration of atazanavir into an existing liquid chromatography UV method for protease inhibitors: validation and application, Ther. Drug Monit. 29 (2007) 103–109.
[15] R. Verbesselt, E. van Wijngaerden, J. de Hoon, Simultaneous determination of 8 HIV protease inhibitors in human plasma by isocratic high-performance liquid chromatography with combined use of UV and fluorescence detection: amprenavir, indinavir, atazanavir, ritonavir, lopinavir, saquinavir, nelfinavir and M8-nelfinavir metabolite, J. Chromatogr. B 845 (2007) 51–60.
[16] A. Loregian, S. Pagni, E. Ballarin, E. Sinigalia, S.G. Parisi, G. Palu, Simple determination of the HIV protease inhibitor atazanavir in human plasma by high-performance liquid chromatography with UV detection, J. Pharm. Biomed. Anal. 42 (2006) 500–505.
[17] N.L. Rezk, R.D. Crutchley, R.F. Yeh, A.D.M. Kashuba, Full validation of an analytical method for the HIV-protease inhibitor atazanavir in combination with 8 other antiretroviral agents and its applicability to therapeutic drug monitoring, Ther. Drug Monit. 28 (2006) 517–525.
[18] R.W. Sparidans, F. Dost, K.M.L. Crommentuyn, A.D.R. Huitema, J.H.M. Schellens, J.H. Beijnen, Liquid chromatographic assay for the protease inhibitor atazanavir in plasma, Biomed. Chromatogr. 20 (2006) 72–76.
[19] E. Cateau, N. Tornier, A. Dupuis, G. le Moal, N. Venisse, Determination of atazanavir in human plasma using solid-phase extraction and high-performance liquid chromatography, J. Pharm. Biomed. Anal. 39 (2005) 791–795.
[20] O. Tribut, M.C. Verdier, C. Arvieux, H. Allain, C. Michelet, D. Bentue-Ferrer, Simultaneous quantitative assay of atazanavir and 6 other HIV protease inhibitors by isocratic reversed-phase liquid chromatography in human plasma, Ther. Drug Monit. 27 (2005) 265–269.
[21] J.M. Poirier, P. Robidou, P. Jaillon, Simple and simultaneous determination of the HIV-protease inhibitors amprenavir, atazanavir, indinavir, lopinavir, nelfinavir, ritonavir, and saquinavir, plus M8 nelfinavir metabolite and the non-nucleoside reverse transcriptase inhibitors efavirenz and nevirapine in human plasma by reversed-phase liquid chromatography, Ther. Drug Monit. 27 (2005) 186–192.
[22] E. Dailly, F. Raffi, P. Jolliet, Determination of atazanavir and other antiretroviral drugs (indinavir, amprenavir, nelfinavir and its active metabolite M8, saquinavir, ritonavir, lopinavir, nevirapine and efavirenz), J. Chromatogr. B 813 (2004) 353–358.
[23] S. Colombo, N. Guignard, C. Marzolini, A. Telenti, J. Biollaz, L.A. Decosterd, Determination of the new HIV-protease inhibitor atazanavir by liquid chromatography after solid-phase extraction, J. Chromatogr. B 810 (2004) 25–34.
[24] ICH Guideline, Stability Testing of New Drug Substances and Drug Products, Q1A (R2), 6 February, 2003.
[25] ICH Guideline, Impurities in New Drug Substances, Q3A (R2), October 25, 2006.
[26] ICH Guideline, Good Manufacturing Practice Guide for Active Pharmaceutical Ingredients, Q7, November 2000.
[27] ICH Guideline, Q2 (R1), Validation of Analytical Procedures, Text and Methodology, November 2005.
[28] Z. Xu, J. Singh, M.D. Schwinden, B. Zheng, T.P. Kissick, B. Patel, M.J. Humora, F. Quiroz, L. Dong, D.M. Hsieh, J.E. Heikes, M. Pudipeddi, M.D. Lindrud, S.K. Srivastava, D.R. Kronenthal, R.H. Mueller, Process research and development for an efficient synthesis of the HIV protease inhibitor BMS-232632, Org. Process Res. Dev. 6 (2002) 323–328.
[29] L.R. Snyder, J.J. Kirkland, J.L. Glajch, Practical HPLC Method Development, 2nd edition, John Wiley & Sons Inc., New York, March 1997.
[30] European Pharmacopeia, 6.4, 2009, Council of Europe, Strasbourg, France, pp. 4407–4413.